

On Fast-Decodable Space–Time Block Codes

Ezio Biglieri

Yi Hong

Emanuele Viterbo

Abstract

We focus on full-rate, fast-decodable space–time block codes (STBCs) for 2×2 and 4×2 multiple-input multiple-output (MIMO) transmission. We first derive conditions for reduced-complexity maximum-likelihood decoding, and apply them to a unified analysis of two families of 2×2 STBCs that were recently proposed. In particular, we describe a reduced-complexity sphere decoding algorithm suitable for QAM signal constellations. Next, we derive a novel reduced-complexity 4×2 STBC, and show that it outperforms all previously known codes with certain constellations.

Index Terms

Alamouti code, quasi-orthogonal space–time block codes, sphere decoder, multiple-input multiple-output.

I. INTRODUCTION

In 1998, Alamouti [1] invented a remarkable scheme for multiple-input multiple-output (MIMO) transmission using two transmit antennas. Thanks to its orthogonality properties, this scheme admits a low-complexity maximum-likelihood (ML) decoder. Motivated by the Alamouti code, *space–time block codes* (STBCs) using more than two transmit antennas for communication over Rayleigh fading channels were introduced in [20] by using the theory of *generalized orthogonal designs*. For such codes, ML decoding is achieved in a simple way through decoupling of the signals transmitted from different antennas rather than by joint detection. Orthogonal STBCs were specifically designed in [20] to achieve the maximum diversity gain [6, 21] for a given

Ezio Biglieri is with Departament de Tecnologies de la Informació i les Comunicacions, Universitat Pompeu Fabra (DTIC-UPF), Barcelona, Spain. E-mail: e.biglieri@ieee.org. Emanuele Viterbo and Yi Hong are with DEIS - Università Della Calabria, via P. Bucci, 42/C, 87036 Rende (CS), Italy. E-mail: {viterbo,hong}@deis.unical.it. This work was supported by the STREP project No. IST-026905 (MASCOT) within the Sixth Framework Programme of the European Commission. Ezio Biglieri's work was also supported by Sequans Communications, Paris.

number of transmit and receive antennas, subject to the constraint of simple ML decoding. It was also proved in [20] that, for more than two antennas, full transmission rate is not achievable with orthogonal STBCs.

Subsequent work includes quasi-orthogonal space–time block codes [11] and algebraic space–time block codes [2, 5, 7, 13, 18]. The proposed quasi-orthogonal STBCs in [11] can support a transmission rate larger than orthogonal STBCs, but at the price of a smaller diversity gain. Using algebraic number theory and cyclic division algebras, algebraic STBCs can be designed to achieve full rate and full diversity, but at the price of a higher decoding complexity.

Recently, a family of full-rate, full-diversity STBCs for 2×2 MIMO was proposed in [9, 10, 22, 23] using a combination of *Clifford-algebra* and Alamouti structures, namely *twisted space–time transmit diversity* code. Specifically, the codeword matrix can be expressed as a combination of two matrices, one with Alamouti structure and one with a Clifford-algebra structure. This family was recently rediscovered in [15], where it was also pointed out that such STBCs enable reduced-complexity ML decoding (see *infra* for a definition of decoding complexity). Independently, the same STBCs were found in [16], and classified under the rubric of *multi-strata* space–time codes. More recently, another family of full-rate, full-diversity, fast-decodable STBCs for 2×2 MIMO was proposed in [19]. This family of STBCs employs a combination of two different rotated Alamouti codewords.

Although a full understanding of the tradeoff among rate, error rate, and decoding complexity of STBCs is still elusive, empirical evidence seems to show that the constraint of simplified ML decoding (to be defined below) does not entail substantial performance loss. To substantiate the above claim, the present paper provides a unified view of the fast-decodable STBCs in [9, 15, 16, 19, 22, 23]. In particular, we study systematically both families of full-rate, full-diversity, fast-decodable STBCs for 2×2 MIMO. We show that these families enable the same low-complexity ML decoding procedure, and we specialize it in the form of a sphere-decoder (SD) search [4, 17, 24, 25]. We also derive general design criteria for full-rate, fast-decodable STBCs, and we exhibit the design of a family of 4×2 codes based on a combination of algebraic and quasi-orthogonal structures, and enabling reduced-complexity ML decoding. In this case, the full diversity assumption will be dropped. Within this family, we show a code that outperforms all previously proposed 4×2 STBCs for 4-QAM signal constellation.

The balance of this paper is organized as follows. Section II introduces system model and

code design criteria. In Section III we review two families of fast-decodable STBCs recently appeared in the literature for 2×2 MIMO. In Section IV, we show how both families of STBCs enable a reduced-complexity ML decoding procedure, and we discuss a low-complexity decoding algorithm. Next, we generalize the design criteria of 2×2 fast-decodable STBCs. In Section V, we examine fast-decodable 4×2 STBCs. A new code is found which outperforms any known 4×2 STBC. In Section VI, we explain how such STBCs enable low-complexity ML decoding, and we develop the corresponding SD algorithm. Finally, conclusions are drawn in Section VII.

A. Notations

Boldface letters are used for column vectors, and capital boldface letters for matrices. Superscripts T , \dagger , and $*$ denote transposition, Hermitian transposition, and complex conjugation, respectively. \mathbb{Z} , \mathbb{C} , and $\mathbb{Z}[j]$ denote the ring of rational integers, the field of complex numbers, and the ring of Gaussian integers, respectively, where $j^2 = -1$. Also, \mathbf{I}_n denotes the $n \times n$ identity matrix, and $\mathbf{0}_{m \times n}$ denotes the $m \times n$ matrix all of whose elements are 0.

Given a complex number x we define the $(\check{\cdot})$ operator from \mathbb{C} to \mathbb{R}^2 as

$$\check{x} \triangleq [\Re(x), \Im(x)]^T$$

where $\Re(\cdot)$ and $\Im(\cdot)$ denote real and imaginary parts. The $(\check{\cdot})$ operator can be extended to complex vectors $\mathbf{x} = [x_1, \dots, x_n] \in \mathbb{C}^n$ as

$$\check{\mathbf{x}} \triangleq [\Re(x_1), \Im(x_1), \dots, \Re(x_n), \Im(x_n)]^T$$

Given a complex number x , the $(\check{\cdot})$ operator from \mathbb{C} to $\mathbb{R}^{2 \times 2}$ is defined by

$$\check{x} \triangleq \begin{bmatrix} \Re(x) & -\Im(x) \\ \Im(x) & \Re(x) \end{bmatrix}$$

The $(\check{\cdot})$ operator can be similarly extended to $n \times n$ matrices by applying it to all the entries, which yields $2n \times 2n$ real matrices. The following relations hold:

$$\widetilde{\mathbf{A}\mathbf{x}} = \check{\mathbf{A}}\check{\mathbf{x}}$$

and

$$\mathbf{A} = \mathbf{B}\mathbf{C} \implies \check{\mathbf{A}} = \check{\mathbf{B}}\check{\mathbf{C}}$$

Given a complex number x , we define the $(\bar{\cdot})$ operator from \mathbb{C} to $\mathbb{R}^{2 \times 2}$ as

$$\bar{x} \triangleq \begin{bmatrix} -\Re(x) & -\Im(x) \\ -\Im(x) & \Re(x) \end{bmatrix}$$

The following relation holds:

$$\widetilde{xy^*} \triangleq \bar{x} \cdot \tilde{y}$$

The $\text{vec}(\cdot)$ operator stacks the m column vectors of a $n \times m$ complex matrix into a mn complex column vector. The $\|\cdot\|$ operation denotes the Euclidean norm of a vector. Finally, the Hermitian inner product of two complex column vectors \mathbf{a} and \mathbf{b} is denoted by

$$\langle \mathbf{a}, \mathbf{b} \rangle \triangleq \mathbf{a}^T \mathbf{b}^*$$

Note also that if $\langle \mathbf{a}, \mathbf{b} \rangle = 0$, then $\langle \tilde{\mathbf{a}}, \tilde{\mathbf{b}} \rangle = 0$.

II. SYSTEM MODEL AND CODE DESIGN CRITERIA

We consider a $n_r \times n_t$ MIMO transmission over a block-fading channel. The received signal matrix $\mathbf{Y} \in \mathbb{C}^{n_r \times T}$ is given by

$$\mathbf{Y} = \mathbf{H}\mathbf{X} + \mathbf{N} \quad (1)$$

where $\mathbf{X} \in \mathbb{C}^{n_t \times T}$ is the codeword matrix, transmitted over T channel uses. Moreover, $\mathbf{N} \in \mathbb{C}^{n_r \times T}$ is a complex white Gaussian noise with i.i.d. entries $\sim \mathcal{N}_{\mathbb{C}}(0, N_0)$, and $\mathbf{H} = [h_{il}] \in \mathbb{C}^{n_r \times n_t}$ is the channel matrix, assumed to remain constant during the transmission of a codeword, and to take on independent values from codeword to codeword. The elements of \mathbf{H} are assumed to be i.i.d. circularly symmetric Gaussian random variables $\sim \mathcal{N}_{\mathbb{C}}(0, 1)$. The realization of \mathbf{H} is assumed to be known at the receiver, but not at the transmitter.

The following definitions are relevant here:

Definition 1: (Code rate) The code rate of a STBC is defined as the number κ of independent information symbols per codeword, drawn from a complex constellation \mathcal{S} . If $\kappa = n_r T$, the STBC is said to have *full rate*. \square

Consider now ML decoding. This consists of finding the code matrix \mathbf{X} that achieves the minimum of the squared Frobenius norm $m(\mathbf{X}) \triangleq \|\mathbf{Y} - \mathbf{H}\mathbf{X}\|^2$.

Definition 2: (Decoding Complexity) The ML decoding complexity can be measured by counting the minimum number of values of $m(\mathbf{X})$ that should be computed in ML decoding.

This number cannot exceed M^κ , with $M = |\mathcal{S}|$, the worst-case decoding complexity achieved by an exhaustive-search ML decoder. \square

Definition 3: (Simplified decoding) We say that a STBC admits simplified decoding if ML decoding can be achieved with less than M^κ computations of $m(\mathbf{X})$. \square

Assuming that a codeword \mathbf{X} is transmitted, it may occur that $\|\mathbf{Y} - \mathbf{H}\mathbf{X}\|^2 > \|\mathbf{Y} - \mathbf{H}\hat{\mathbf{X}}\|^2$, with $\hat{\mathbf{X}} \neq \mathbf{X}$, resulting in a *pairwise error*. Let r denote the rank of the *codeword-difference matrix* $\mathbf{X} - \hat{\mathbf{X}}$, with $\mathbf{X} \neq \hat{\mathbf{X}}$, and let $\mathbf{E} \triangleq (\mathbf{X} - \hat{\mathbf{X}})(\mathbf{X} - \hat{\mathbf{X}})^\dagger$ be the *codeword-distance matrix*. Let δ denote the *product distance*, i.e., the product of non-zero eigenvalues of the codeword distance matrix \mathbf{E} . The error probability of a STBC is upper bounded by the following union bound,

$$\begin{aligned} P(e) &\leq \frac{1}{M^\kappa} \sum_{\mathbf{X}} \sum_{\mathbf{X} \neq \hat{\mathbf{X}}} P(\mathbf{X} \rightarrow \hat{\mathbf{X}}) \\ &= \frac{1}{M^\kappa} \sum_r \sum_\delta A(r, \delta) P(r, \delta) \end{aligned} \quad (2)$$

where $P(\mathbf{X} \rightarrow \hat{\mathbf{X}})$ denotes the pairwise error probability (PEP) among distinct pairs $(\mathbf{X}, \hat{\mathbf{X}})$. The term $P(r, \delta)$ represents the PEP of the codewords with rank r and product distance δ , while $A(r, \delta)$ denotes the associated multiplicity.

Definition 4: (Full-diversity STBC) A full-diversity STBC is one with $r = n_t$ over all possible codeword-difference matrices. \square

For a full-diversity STBC, the worst-case PEP depends asymptotically, for high signal-to-noise ratios, on both the rank $r = n_t$ and the *minimum determinant* of the codeword distance matrix

$$\delta_{\min} \triangleq \min_{\mathbf{X} \neq \hat{\mathbf{X}}} \det(\mathbf{E})$$

The “rank-and-determinant criterion” (RDC) of code design requires the maximization of both r and δ_{\min} . This criterion yields *diversity gain* $n_r n_t$ and *coding gain* $(\delta_{\min})^{1/n_t}$ [21].

For a non full-diversity STBC, the minimum determinant equals to zero. In such a case, we have to minimize the associated multiplicity of the *dominant pairwise terms* of rank $r \leq n_t$ independently of their product distance.

A. Linear codes

We consider now the subclass of *linear* STBCs, which are especially relevant in our context because they admit ML sphere decoding.

Definition 5: (Linear STBC) A STBC carrying κ symbols $\mathbf{s} = [s_1, \dots, s_\kappa]$ is said to be (*real*) *linear* if we can write

$$\widetilde{\text{vec}}(\mathbf{X}) = \mathbb{G}\tilde{\mathbf{s}}$$

for some $\mathbb{G} \in \mathbb{R}^{2n_t T \times 2\kappa}$. The matrix \mathbb{G} is called the (*real*) *generator matrix* of the linear code. If a complex matrix $\mathbf{G} \in \mathbb{C}^{n_t T \times \kappa}$ exists such that $\mathbb{G} = \check{\mathbf{G}}$, then we can write

$$\text{vec}(\mathbf{X}) = \mathbf{G}\mathbf{s}$$

which identifies a *complex linear* STBC, with \mathbf{G} its *complex generator matrix*. □

For example, the following STBC is complex linear:

$$\mathbf{X} = \begin{bmatrix} s_1 & -s_2 \\ s_2 & s_1 \end{bmatrix} \implies \text{vec}(\mathbf{X}) = \mathbf{G}\mathbf{s} = \begin{bmatrix} 1 & 0 \\ 0 & 1 \\ 0 & -1 \\ 1 & 0 \end{bmatrix} \begin{bmatrix} s_1 \\ s_2 \end{bmatrix}$$

The Alamouti code:

$$\mathbf{X} = \begin{bmatrix} s_1 & -s_2^* \\ s_2 & s_1^* \end{bmatrix} \implies \widetilde{\text{vec}}(\mathbf{X}) = \mathbb{G}\tilde{\mathbf{s}}$$

is a linear STBC, but not complex linear, because no \mathbf{G} exists such that $\mathbb{G} \neq \check{\mathbf{G}}$.

Definition 6: (Cubic shaping) If the generator matrix of a linear code satisfies $\mathbb{G}^\dagger \mathbb{G} = \mathbf{I}_{2\kappa}$, then we say that the STBC *has cubic shaping* (or that *is information-lossless*). It is known that cubic shaping is especially desirable for high-dimensional signal constellations [14]. □

It can be proved that a linear STBC admits the canonical decomposition

$$\mathbf{X} = \sum_{\ell=1}^{\kappa} (a_\ell \mathbf{A}_\ell + j b_\ell \mathbf{B}_\ell) \tag{3}$$

where a_ℓ and b_ℓ are the real and imaginary part of s_ℓ , respectively, and $\mathbf{A}_\ell, \mathbf{B}_\ell, \ell = 1, \dots, \kappa$, are $n_t \times T$ (generally complex) matrices. With this decomposition, we may also rephrase (1) using only real quantities: explicitly,

$$\widetilde{\text{vec}}(\mathbf{Y}) = \mathbb{F}\tilde{\mathbf{s}} + \widetilde{\text{vec}}(\mathbf{N}) \tag{4}$$

where

$$\mathbb{F} \triangleq [\widetilde{\text{vec}}(\mathbf{H}\mathbf{A}_1), \widetilde{\text{vec}}(\mathbf{H}\mathbf{B}_1), \dots, \widetilde{\text{vec}}(\mathbf{H}\mathbf{B}_\kappa)] = \text{diag}(\check{\mathbf{H}}, \dots, \check{\mathbf{H}}) \mathbb{G}$$

and $\mathbb{G} = [\widetilde{\text{vec}(\mathbf{A}_1)}, \dots, \widetilde{\text{vec}(\mathbf{B}_\kappa)}]$. Note that the \mathbb{F} matrix depends on \mathbf{H} . In the case of complex linear STBC, we may use only complex quantities:

$$\text{vec}(\mathbf{Y}) = \mathbf{F}\mathbf{s} + \text{vec}(\mathbf{N}) \quad (5)$$

where now

$$\mathbf{F} \triangleq [\text{vec}(\mathbf{H}\mathbf{A}_1), \text{vec}(\mathbf{H}\mathbf{B}_1), \dots, \text{vec}(\mathbf{H}\mathbf{B}_\kappa)] = \text{diag}(\mathbf{H}, \dots, \mathbf{H}) \mathbf{G} \quad (6)$$

with $\mathbf{G} = [\text{vec}(\mathbf{A}_1), \dots, \text{vec}(\mathbf{B}_\kappa)]$, $\check{\mathbf{G}} = \mathbb{G}$, and $\check{\mathbf{F}} = \mathbb{F}$.

Definition 7: (Matched-filter receiver) Premultiplying the received vector $\widetilde{\text{vec}(\mathbf{Y})}$ by the "matched filter" \mathbb{F}^T [12], we obtain a real vector with 2κ components corresponding to a sufficient statistic to estimate \mathbf{s} . The matched-filter (MF) receiver is one making symbol-by-symbol decisions on these components. Notice that, whenever $\mathbb{F}^T\mathbb{F} = \mathbf{I}$, the MF receiver yields ML decoding. \square

Definition 8: (ML decoding with QR decomposition) Compute the QR decomposition $\mathbb{F} = \mathbf{Q}\mathbf{R}$, where \mathbf{Q} is orthogonal and \mathbf{R} is upper triangular. ML decoding is equivalent to minimizing $\|\mathbf{Q}^T \widetilde{\text{vec}(\mathbf{Y})} - \mathbf{R}\tilde{\mathbf{s}}\|$. \square

B. Codes with the Alamouti structure.

Definition 9: (Alamouti structure) We say that a STBC has the *Alamouti structure* if

$$\mathbf{X} = \begin{bmatrix} \alpha s_1 & -\beta s_2^* \\ \alpha s_2 & \beta s_1^* \end{bmatrix} \quad (7)$$

where $s_i \in \mathbb{C}$ with $i = 1, 2$, and $\alpha, \beta \in \mathbb{C}$, $|\alpha|^2 = |\beta|^2$, and $|\alpha|^2 + |\beta|^2 = 1$. \square

For a code with the Alamouti structure, we have

$$\mathbf{A}_1 \triangleq \begin{bmatrix} \alpha & 0 \\ 0 & \beta \end{bmatrix} \quad \mathbf{B}_1 \triangleq \begin{bmatrix} \alpha & 0 \\ 0 & -\beta \end{bmatrix} \quad (8)$$

$$\mathbf{A}_2 \triangleq \begin{bmatrix} 0 & -\beta \\ \alpha & 0 \end{bmatrix} \quad \mathbf{B}_2 \triangleq \begin{bmatrix} 0 & \beta \\ \alpha & 0 \end{bmatrix} \quad (9)$$

and hence, defining $\alpha = \alpha' + j\alpha''$, and $\beta = \beta' + j\beta''$,

$$\mathbb{G} = \begin{bmatrix} \alpha' & -\alpha'' & 0 & 0 \\ \alpha'' & \alpha' & 0 & 0 \\ 0 & 0 & \alpha' & -\alpha'' \\ 0 & 0 & \alpha'' & \alpha' \\ 0 & 0 & -\beta' & -\beta'' \\ 0 & 0 & -\beta'' & \beta' \\ \beta' & \beta'' & 0 & 0 \\ \beta'' & -\beta' & 0 & 0 \end{bmatrix} = \begin{bmatrix} \check{\alpha} & \check{\check{0}} \\ \check{\check{0}} & \check{\alpha} \\ \check{\check{0}} & \check{\check{\beta}} \\ -\check{\check{\beta}} & \check{\check{0}} \end{bmatrix} \quad (10)$$

We can see, by direct calculation, that $\mathbb{G}^T \mathbb{G} = \mathbf{I}_4$. Moreover, given $\mathbf{H} = [h_{ij}] \in \mathbb{C}^{2 \times 2}$ and $\mathbf{Y} = [y_{ij}] \in \mathbb{C}^{2 \times 2}$, let us define

$$\begin{aligned} \mathbf{y} &\triangleq [y_{11}, y_{21}, y_{12}^*, y_{22}^*]^T \\ \mathbf{n} &\triangleq [n_{11}, n_{21}, n_{12}^*, n_{22}^*]^T \end{aligned} \quad (11)$$

where the last two elements of the vectorized matrices are conjugated. We can write

$$\mathbf{y} = \mathbf{F}^{(*)} \mathbf{s} + \mathbf{n} \quad (12)$$

where

$$\mathbf{F}^{(*)} = [\mathbf{f}_1 | \mathbf{f}_2] = \begin{bmatrix} \alpha h_{11} & \alpha h_{12} \\ \alpha h_{21} & \alpha h_{22} \\ \beta^* h_{12}^* & -\beta^* h_{11}^* \\ \beta^* h_{22}^* & -\beta^* h_{21}^* \end{bmatrix} \quad \text{and} \quad \check{\mathbb{F}} \triangleq \check{\mathbf{F}}^{(*)} = [\check{\mathbf{f}}_1 | \check{\mathbf{f}}_2] \quad (13)$$

Note that $\mathbf{F}^{(*)}$ has its last two rows conjugated. In complex notations, multiplication of \mathbf{y} by $(\mathbf{F}^{(*)})^\dagger$ is equivalent to matched filtering. Direct calculation shows that, for codes with the Alamouti structure, $\mathbf{F}^{(*)\dagger} \mathbf{F}^{(*)} = \mathbf{I}_2$ (or $\check{\mathbb{F}}^T \check{\mathbb{F}} = \mathbf{I}_4$). Consequently, ML decoding can be done symbol-by-symbol, which, under our definition, yields a complexity $2M$.

III. FAST-DECODABLE CODES FOR 2×2 MIMO

Consider now 2×2 STBCs. These are full-rate and full-diversity if $\kappa = 4$ symbols/codeword and $r = n_t$.

Definition 10: (Fast-decodable STBCs for 2×2 MIMO) A 2×2 STBC allows fast ML decoding if its complexity does not exceed $2M^3$. \square

Here we examine 2×2 fast-decodable STBCs endowed with the following structure: consider the sum code

$$\mathbf{X} = \mathbf{X}_{1,2}(s_1, s_2) + \mathbf{X}_{3,4}(s_3, s_4) \quad (14)$$

where the first (resp., second) component code encodes symbols s_1, s_2 (resp., s_3, s_4). The idea here is to achieve simplified decoding by choosing $\mathbf{X}_{1,2}$ as an Alamouti code (since it has the lowest complexity), and $\mathbf{X}_{3,4}$ so that its decoding is in some way “decoupled” from that of $\mathbf{X}_{1,2}$. Two implementations of this idea have been recently presented in the literature, as summarized below within our conceptual framework.

A. Family I

In the first family of fast-decodable STBCs, independently derived in [15, 16, 23], $\mathbf{X}_{3,4}(s_3, s_4)$ is chosen as follows: let

$$\mathbf{T} \triangleq \begin{bmatrix} 1 & 0 \\ 0 & -1 \end{bmatrix} \quad \text{and} \quad \begin{bmatrix} z_1 \\ z_2 \end{bmatrix} = \mathbf{U} \begin{bmatrix} s_3 \\ s_4 \end{bmatrix} \quad (15)$$

where $z_1, z_2 \in \mathbb{C}$, and $\mathbf{U} \in \mathbb{C}^{2 \times 2}$ is the unitary “Alamouti” matrix

$$\mathbf{U} = \begin{bmatrix} \varphi_1 & -\varphi_2^* \\ \varphi_2 & \varphi_1^* \end{bmatrix}$$

with $|\varphi_1|^2 + |\varphi_2|^2 = 1$. We have

$$\mathbf{X}_{3,4}(s_3, s_4) = \mathbf{T} \begin{bmatrix} z_1 & -z_2^* \\ z_2 & z_1^* \end{bmatrix} = \begin{bmatrix} \varphi_1 s_3 - \varphi_2^* s_4 & -(\varphi_2 s_3 + \varphi_1^* s_4)^* \\ \varphi_2 s_3 + \varphi_1^* s_4 & (\varphi_1 s_3 - \varphi_2^* s_4)^* \end{bmatrix} \quad (16)$$

which has the Alamouti structure (7). Vectorizing, and separating real and imaginary parts of the matrix \mathbf{X} , we obtain

$$\widetilde{\text{vec}}(\mathbf{X}) = \mathbb{G} [\tilde{s}_1, \tilde{s}_2, \tilde{s}_3, \tilde{s}_4]^T = \mathbb{G}_1 [\tilde{s}_1, \tilde{s}_2]^T + \mathbb{G}_2 [\tilde{s}_3, \tilde{s}_4]^T$$

Thus, $\mathbb{G} = [\mathbb{G}_1, \mathbb{G}_2] \in \mathbb{R}^{8 \times 8}$ is the generator matrix of the code. Specifically, $\mathbb{G}_1 \in \mathbb{R}^{8 \times 4}$ is the generator matrix of $\mathbf{X}_{1,2}$, and $\mathbb{G}_2 \in \mathbb{R}^{8 \times 4}$ is the generator matrix of $\mathbf{X}_{3,4}$. The matrix \mathbb{G}_1 has the

structure of (10) with coefficients $\alpha_{1,2}$ and $\beta_{1,2}$:

$$\mathbb{G}_1 \triangleq [\mathbf{g}_1 \mid \mathbf{g}_2 \mid \mathbf{g}_3 \mid \mathbf{g}_4] \triangleq \begin{bmatrix} \check{\alpha}_{1,2} & \check{0} \\ \check{0} & \check{\alpha}_{1,2} \\ \check{0} & \check{\beta}_{1,2} \\ -\check{\beta}_{1,2} & \check{0} \end{bmatrix} \quad (17)$$

while

$$\mathbb{G}_2 \triangleq [\mathbf{g}_5 \mid \mathbf{g}_6 \mid \mathbf{g}_7 \mid \mathbf{g}_8] \triangleq \begin{bmatrix} \check{\varphi}_1 & -\check{\varphi}_2^* \\ -\check{\varphi}_2 & -\check{\varphi}_1^* \\ \check{\varphi}_2^* & \check{\varphi}_1 \\ \check{\varphi}_1^* & -\check{\varphi}_2 \end{bmatrix} \quad (18)$$

Direct computation shows that \mathbb{G}_1 and \mathbb{G}_2 have the following properties:

Property 1: (Column orthogonality) Both \mathbb{G}_1 and \mathbb{G}_2 have orthogonal columns: $\langle \mathbf{g}_i, \mathbf{g}_j \rangle = 0$, where $i, j \in [1, 4]$ or $i, j \in [5, 8]$. \square

Property 2: (Mutual column orthogonality) With \mathbf{T} as in (15), the subspace spanned by the columns of \mathbb{G}_2 is orthogonal to the one spanned by the columns of \mathbb{G}_1 , i.e., $\langle \mathbf{g}_i, \mathbf{g}_j \rangle = 0$, for $i \in [1, 4]$ and $j \in [5, 8]$. \square

Property 3: (Cubic shaping) As a consequence of the two previous properties, $\mathbb{G}^\dagger \mathbb{G} = \mathbf{I}_8$, which implies cubic shaping. \square

The matrix \mathbf{U} should be chosen so as to achieve full rank and maximize the minimum determinant. The best known code of the form (14) was first found in [23]. It is defined by the following unitary matrix:

$$\mathbf{U} = \frac{1}{\sqrt{7}} \begin{bmatrix} 1+j & -1+2j \\ 1+2j & 1-j \end{bmatrix}$$

This code was independently rediscovered in [15] and [16] by numerical optimization. Its minimum determinants under different signal constellations are shown in Table I.

B. Family II

In the second family of fast-decodable STBCs [19], both $\mathbf{X}_{1,2}(s_1, s_2)$ and $\mathbf{X}_{3,4}(s_3, s_4)$ have the Alamouti structure (7), with coefficients $\alpha_{1,2}, \beta_{1,2}$ used for $\mathbf{X}_{1,2}(s_1, s_2)$, and $\alpha_{3,4}, \beta_{3,4}$ for $\mathbf{X}_{3,4}(s_3, s_4)$. Vectorizing and separating real and imaginary parts of the matrices \mathbf{X} , we obtain

for both $\mathbf{X}_{1,2}$ and $\mathbf{X}_{3,4}$ the same generator matrices as in (17)-(18). However, if we compare Family II with Family I, we can see that the former STBCs satisfy Property 1, but not Properties 2 and 3. This is due to the fact that the columns of \mathbb{G}_1 and \mathbb{G}_2 are not orthogonal to each other, and hence $\mathbb{G}^\dagger \mathbb{G} \neq \mathbf{I}_8$. This implies that the STBCs of Family II do not have cubic shaping.

The best known code in this family, proposed in [19], has parameters

$$\alpha_{1,2} = 1/\sqrt{2}, \quad \beta_{1,2} = e^{0.635\pi j}/\sqrt{2}, \quad \alpha_{3,4} = e^{0.3438\pi j}/\sqrt{2}, \quad \beta_{3,4} = e^{0.4788\pi j}/\sqrt{2}$$

C. Comparing the two families

Table I compares the minimum determinant δ_{\min} of the best known STBCs in the two families with that of the Golden code for 4-, 16- and 64-QAM signaling, respectively. In the computation, we assume that the constellation points are lying on the odd integers. It can be seen that the minimum determinants of Family-I STBCs and of the Golden code are constant, while the minimum determinant of Family-II STBC decreases slowly as the size of the signal constellation increases. Furthermore, the codes of [15, 16, 23] have larger minimum determinants than that of [19].

Let us define the signal-to-noise ratio (SNR) as $\text{SNR} \triangleq n_t E_s / N_0$, where E_s the average energy. Figs. 1 and 2 compare the codeword error rate (CER) of the best STBCs in the two families and of the Golden code with 4- and 16-QAM signaling, respectively. It is shown that both families of STBCs exhibit similar CER performance, and a small difference, at high SNR, with the Golden code. Since the latter has the best CER known, but does not admit simplified decoding, this difference can be interpreted as the penalty to be paid for complexity reduction.

IV. DECODING FAMILY-I AND II STBCS

In this section we elaborate on the decoding complexity of codes in Families I and II. We first provide a simple but general analysis, next we focus on sphere detection, and describe a decoding algorithm aimed at QAM signals.

A. General decoding with QR decomposition

Consider (12), and ML decoding with QR decomposition of $\mathbf{F}^{(*)}$. This consists of minimizing $\|\mathbf{Q}^\dagger \mathbf{y} - \mathbf{R}\mathbf{s}\|^2$, where $\mathbf{F}^{(*)} = \mathbf{Q}\mathbf{R}$, $\mathbf{Q} \in \mathbb{C}^{4 \times 4}$ is unitary, $\mathbf{R} \in \mathbb{C}^{4 \times 4}$ is upper-triangular. If we

write

$$\mathbf{F}^{(*)} = [\mathbf{f}_1 \mid \mathbf{f}_2 \mid \mathbf{f}_3 \mid \mathbf{f}_4] \in \mathbb{C}^{4 \times 4}$$

then the matrices \mathbf{Q} and \mathbf{R} have the general form

$$\mathbf{Q} = [\mathbf{e}_1 \mid \mathbf{e}_2 \mid \mathbf{e}_3 \mid \mathbf{e}_4]$$

and

$$\mathbf{R} = \begin{bmatrix} \|\mathbf{d}_1\| & \langle \mathbf{f}_2, \mathbf{e}_1 \rangle & \langle \mathbf{f}_3, \mathbf{e}_1 \rangle & \langle \mathbf{f}_4, \mathbf{e}_1 \rangle \\ 0 & \|\mathbf{d}_2\| & \langle \mathbf{f}_3, \mathbf{e}_2 \rangle & \langle \mathbf{f}_4, \mathbf{e}_2 \rangle \\ 0 & 0 & \|\mathbf{d}_3\| & \langle \mathbf{f}_4, \mathbf{e}_3 \rangle \\ 0 & 0 & 0 & \|\mathbf{d}_4\| \end{bmatrix}$$

where

$$\begin{aligned} \mathbf{d}_1 &= \mathbf{f}_1 & \mathbf{e}_1 &= \frac{\mathbf{d}_1}{\|\mathbf{d}_1\|} = \frac{\mathbf{f}_1}{\|\mathbf{f}_1\|} \\ \mathbf{d}_i &= \mathbf{f}_i - \sum_{j=1}^{i-1} \text{Proj}_{\mathbf{e}_j} \mathbf{f}_i & \mathbf{e}_i &= \frac{\mathbf{d}_i}{\|\mathbf{d}_i\|}, \quad i = 2, \dots, 4 \end{aligned}$$

and $\text{Proj}_{\mathbf{u}} \mathbf{v} \triangleq \frac{\langle \mathbf{v}, \mathbf{u} \rangle}{\langle \mathbf{u}, \mathbf{u} \rangle} \mathbf{u}$.¹

Explicitly, we have, for Family I,

$$\mathbf{F}^{(*)} = [\mathbf{F}_1 \mid \mathbf{F}_2]$$

with $\mathbf{F}_1 \triangleq [\mathbf{f}_1 \mid \mathbf{f}_2]$ having the structure (13) with coefficients $\alpha = \alpha_{1,2}$ and $\beta = \beta_{1,2}$. Moreover,

$$\mathbf{F}_2 \triangleq [\mathbf{f}_3 \mid \mathbf{f}_4] = \begin{bmatrix} A & -B \\ C & -D \\ -B^* & -A^* \\ -D^* & -C^* \end{bmatrix} \quad (19)$$

where

$$\begin{aligned} A &= h_{11}\varphi_1 - h_{12}\varphi_2 & B &= h_{11}\varphi_2^* + h_{12}\varphi_1^* \\ C &= h_{21}\varphi_1 - h_{22}\varphi_2 & D &= h_{21}\varphi_2^* + h_{22}\varphi_1^* \end{aligned} \quad (20)$$

¹This formulation of the QR decomposition coincides with the Gram-Schmidt procedure applied to the column vectors of $\mathbf{F}^{(*)}$.

For Family II we obtain

$$\mathbf{F}^{(*)} \triangleq [\mathbf{f}_1 \mid \mathbf{f}_2 \mid \mathbf{f}_3 \mid \mathbf{f}_4] = \begin{bmatrix} \alpha_{1,2}h_{11} & \alpha_{1,2}h_{12} & \alpha_{3,4}h_{11} & \alpha_{3,4}h_{12} \\ \alpha_{1,2}h_{21} & \alpha_{1,2}h_{22} & \alpha_{3,4}h_{21} & \alpha_{3,4}h_{22} \\ \beta_{1,2}^*h_{12}^* & -\beta_{1,2}^*h_{11}^* & \beta_{3,4}^*h_{12}^* & -\beta_{3,4}^*h_{11}^* \\ \beta_{1,2}^*h_{22}^* & -\beta_{1,2}^*h_{21}^* & \beta_{3,4}^*h_{22}^* & -\beta_{3,4}^*h_{21}^* \end{bmatrix} \quad (21)$$

Now, simplified decoding will be connected to the sparsity of the portion of \mathbf{R} above its main diagonal. Consider first Family I. Direct computation yields

$$\langle \mathbf{f}_1, \mathbf{f}_3 \rangle = \phi_1^* \quad \langle \mathbf{f}_1, \mathbf{f}_4 \rangle = -\phi_2^* \quad \langle \mathbf{f}_2, \mathbf{f}_3 \rangle = \phi_2 \quad \langle \mathbf{f}_2, \mathbf{f}_4 \rangle = \phi_1$$

where $\phi_1 \triangleq \frac{1}{\sqrt{2}}(\rho\varphi_1 - 2c\varphi_2)$, $\phi_2 \triangleq \frac{1}{\sqrt{2}}(\rho\varphi_2^* + 2c\varphi_1^*)$, with $\rho \triangleq |h_{11}|^2 - |h_{12}|^2 + |h_{21}|^2 - |h_{22}|^2$, and $c \triangleq h_{11}^*h_{12} + h_{21}^*h_{22}$. Consequently, \mathbf{R} has the following properties:

- 1) $\langle \mathbf{f}_2, \mathbf{e}_1 \rangle = 0$, $\langle \mathbf{f}_4, \mathbf{e}_3 \rangle = 0$
- 2) $\|\mathbf{d}_1\|^2 = \|\mathbf{d}_2\|^2 \triangleq \mu$, $\|\mathbf{d}_3\|^2 = \|\mathbf{d}_4\|^2 \triangleq \gamma$
- 3) $[\mathbf{e}_1 \mid \mathbf{e}_2] = \frac{1}{\sqrt{\mu}}[\mathbf{f}_1 \mid \mathbf{f}_2] = \frac{1}{\sqrt{\mu}}\mathbf{F}_1$
- 4) Defining

$$\begin{bmatrix} \Phi_1 & \Phi_2 \\ \Phi_3 & \Phi_4 \end{bmatrix} \triangleq \begin{bmatrix} \langle \mathbf{f}_3, \mathbf{e}_1 \rangle & \langle \mathbf{f}_4, \mathbf{e}_1 \rangle \\ \langle \mathbf{f}_3, \mathbf{e}_2 \rangle & \langle \mathbf{f}_4, \mathbf{e}_2 \rangle \end{bmatrix} = \begin{bmatrix} \frac{1}{\sqrt{\mu}}\phi_1 & -\frac{1}{\sqrt{\mu}}\phi_2 \\ \frac{1}{\sqrt{\mu}}\phi_2^* & \frac{1}{\sqrt{\mu}}\phi_1^* \end{bmatrix}$$

$$\text{we have } \Phi_1\Phi_2^* + \Phi_3\Phi_4^* = 0$$

Thus, \mathbf{R} and \mathbf{Q} have the forms

$$\mathbf{R} = \begin{bmatrix} \sqrt{\mu} & 0 & \Phi_1 & \Phi_2 \\ 0 & \sqrt{\mu} & \Phi_3 & \Phi_4 \\ 0 & 0 & \sqrt{\gamma} & 0 \\ 0 & 0 & 0 & \sqrt{\gamma} \end{bmatrix} \quad (22)$$

and $\mathbf{Q} = [\mathbf{Q}_1 \mid \mathbf{Q}_2]$, where

$$\mathbf{Q}_1 \triangleq \frac{1}{\sqrt{\mu}}\mathbf{F}_1 \quad \mathbf{Q}_2 \triangleq [\mathbf{e}_3 \mid \mathbf{e}_4] \quad (23)$$

For Family II, \mathbf{R} has again form (22), where now

$$\begin{aligned}\Phi_1 = \langle \mathbf{f}_3, \mathbf{e}_1 \rangle &= \frac{1}{\sqrt{\mu}} \left[\alpha_{3,4} \alpha_{1,2}^* \left(\sum_{i=1}^2 |h_{i1}|^2 \right) + \beta_{1,2} \alpha_{3,4}^* \left(\sum_{i=1}^2 |h_{i2}|^2 \right) \right] \\ \Phi_2 = \langle \mathbf{f}_4, \mathbf{e}_1 \rangle &= \frac{1}{\sqrt{\mu}} (\alpha_{3,4} \alpha_{1,2}^* - \beta_{1,2} \alpha_{3,4}^*) c \\ \Phi_3 = \langle \mathbf{f}_3, \mathbf{e}_2 \rangle &= \frac{1}{\sqrt{\mu}} (\alpha_{3,4} \alpha_{1,2}^* - \beta_{1,2} \alpha_{3,4}^*) c^* \\ \Phi_4 = \langle \mathbf{f}_4, \mathbf{e}_2 \rangle &= \frac{1}{\sqrt{\mu}} \left[\alpha_{3,4} \alpha_{1,2}^* \left(\sum_{i=1}^2 |h_{i2}|^2 \right) + \beta_{1,2} \alpha_{3,4}^* \left(\sum_{i=1}^2 |h_{i1}|^2 \right) \right]\end{aligned}$$

Examination of the structure of \mathbf{R} in (22) discloses the simplified-decoding property of both families of codes, which admit complexity $2M^3$. In fact, the ML metric turns out to be a sum of four quadratic functions, depending on (s_1, s_3, s_4) , (s_2, s_3, s_4) , s_3 , and s_4 , respectively. This implies that the code can be decoded as follows: choose first a pair (s_3, s_4) . For every such pair (there are M^2 of them) choose separately (possibly, in parallel) s_1 and s_2 so as to minimize the ML metric. Hence, no more than $2M^3$ values of this metric need be computed for simplified ML decoding. In the next subsection, we describe how further simplification of ML decoding can be achieved when the transmitted signals form a square QAM constellation, and SD is used.

B. Sphere decoding

From

$$\mathbf{y} = \mathbf{F}^{(*)} \mathbf{s} + \mathbf{n} = \mathbf{Q} \mathbf{R} \mathbf{s} + \mathbf{n} \quad (24)$$

we obtain

$$\mathbf{r} \triangleq \mathbf{Q}^\dagger \mathbf{y} = \mathbf{R} \mathbf{s} + \mathbf{w} \quad (25)$$

Let $\mathbf{r} = [r_1, \dots, r_4]^T$, and $\mathbf{w} \triangleq \mathbf{Q}^\dagger \mathbf{n} = [w_1, \dots, w_4]^T$. Separating real and imaginary parts in (25), we obtain

$$\tilde{\mathbf{r}} = \tilde{\mathbf{R}} \tilde{\mathbf{s}} + \tilde{\mathbf{w}} \implies \mathbf{v} = \Theta \mathbf{u} + \tilde{\mathbf{w}} \quad (26)$$

where for sake of simplicity we use the following notation:

$$\begin{aligned}\mathbf{v} &= [v_1, \dots, v_8]^T \triangleq \tilde{\mathbf{r}} \\ \mathbf{u} &= [u_1, \dots, u_8]^T \triangleq \tilde{\mathbf{s}}\end{aligned}$$

We now apply SD restricting \mathcal{S} to square QAM constellations, i.e., assuming $u_i \in \mathcal{X}$, where \mathcal{X} is a PAM constellation, so that $\mathcal{S} = \mathcal{X}^2$. SD finds

$$\hat{\mathbf{u}} = \arg \min_{\mathbf{u} \in \mathcal{X}} \|\mathbf{v} - \Theta \mathbf{u}\|^2 \quad (27)$$

where $\hat{\mathbf{u}} = \{\hat{u}_i\}$ with $i = 1, \dots, 8$, and $\hat{u}_i \in \mathcal{X}$. It was pointed out in [4] that the search procedure of a SD can be visualized as a bounded tree search. If *standard* real SD is used for 2×2 STBCs, we have 8 levels of the decoding tree.

Now, the codes examined here allow SD to use only a 4-level tree search. Let us define $\mathbf{u}_i^k \triangleq [u_i, \dots, u_k]^T$, $i < k$, as the partial symbol vector labeling the path connecting level i to level k . In our case, SD is only used to search the branches corresponding to \mathbf{u}_5^8 , while the symbols in \mathbf{u}_1^4 are decoded as in an Alamouti code. We can interpret this complexity reduction by saying that a 4-dimensional real SD can be used *in lieu* of a 8-dimensional real SD.

To use SD to decode \mathbf{u}_5^8 , examine Schnorr-Euchner (SE) enumeration [17]. In general, this starts from the midpoint at level i

$$S_i(u_i) \triangleq \lfloor (v_i - \xi_i) / \theta_{ii} \rfloor \in \mathcal{X}, \quad i = 8, \dots, 5 \quad (28)$$

where $\lfloor \cdot \rfloor$ denotes the closest integer, $\xi_8 = 0$, $S_i(u_i)$ is the ZF-DFE component. ξ_i is the *interference term* on level i from upper level j . Now, due to the property $\langle \mathbf{f}_4, \mathbf{e}_3 \rangle = 0$, the computation of ξ_i in SE enumeration is not necessary, and hence we let $\xi_i = 0$, $5 \leq i \leq 8$.

The SE algorithm visits the neighbors of the midpoint in a zig-zag order. With the definition

$$\Delta_i \triangleq \text{sign}(v_i - \theta_{ii} u_i)$$

where $\text{sign}(a) = +1$ for $a \geq 0$, otherwise $\text{sign}(a) = -1$, Schnorr-Euchner enumeration is used to search

$$u_i = \{S_i(u_i), S_i(u_i) + \Delta_i, S_i(u_i) - \Delta_i, \dots\} \subset \mathcal{X}$$

In this tree search, a branch at level $i \in [5, 8]$ contributes to the ML metric by the amount

$$d_i(\mathbf{u}_5^8) \triangleq |v_i - \theta_{ii} u_i|^2 \quad 5 \leq i \leq 8 \quad (29)$$

The corresponding path metric is given by

$$T_{i-1} \triangleq \sum_{j=i}^8 d_j(\mathbf{u}_j^8) \quad (30)$$

Having determined the partial vector \mathbf{u}_5^8 (corresponding to the decoding level $i = 4$), the property $\langle \mathbf{f}_2, \mathbf{e}_1 \rangle = 0$ in matrix \mathbf{R} allows one to proceed by using symbol-by-symbol "Alamouti" decoding to decode \mathbf{u}_1^4 . We have

$$\begin{aligned}
 u_1 &= \left\lfloor \frac{v_1 - \Re(\Phi_1)u_5 + \Im(\Phi_1)u_6 + \Re(\Phi_2)u_7 - \Im(\Phi_2)u_8}{\mu} \right\rfloor \\
 u_2 &= \left\lfloor \frac{v_2 - \Im(\Phi_1)u_5 - \Re(\Phi_1)u_6 + \Im(\Phi_2)u_7 + \Re(\Phi_2)u_8}{\mu} \right\rfloor \\
 u_3 &= \left\lfloor \frac{v_3 - \Re(\Phi_3)u_5 + \Im(\Phi_3)u_6 + \Re(\Phi_4)u_7 - \Im(\Phi_4)u_8}{\mu} \right\rfloor \\
 u_4 &= \left\lfloor \frac{v_4 - \Im(\Phi_3)u_5 - \Re(\Phi_3)u_6 + \Im(\Phi_4)u_7 + \Re(\Phi_4)u_8}{\mu} \right\rfloor
 \end{aligned} \tag{31}$$

Once \mathbf{u}_1^4 is obtained, a valid vector $\hat{\mathbf{u}} = [\mathbf{u}_1^4 \mid \mathbf{u}_5^8]$ is obtained, which yields the corresponding total path metric T_1 . This completes the search of one path in the 4-dimensional tree. The detailed decoding algorithm is given below.

- 1) (Input) Input Φ_ℓ , $\ell = 1, \dots, 4$, μ , β and γ .
- 2) (Initialization) Set $i = 8$, $T_8 = 0$, and $d_c = C_0$ (current squared radius of the sphere).
- 3) (ZF-DFE on u_i) Set $u_i = \lfloor v_i / \theta_{ii} \rfloor$ and $\Delta_i = \text{sign}(v_i - \theta_{ii}u_i)$.
- 4) (Main step of SD) If $d_c < T_i + |v_i - \theta_{ii}u_i|^2$, then go to Step 5 (outside the sphere).
 Else if $u_i \notin \mathcal{X}$ go to Step 7 (inside the sphere, but outside the signal set).
 Else (inside the sphere, inside the signal set)
 If $i \geq 5$, then $\{ T_{i-1} = T_i + |v_i - \theta_{ii}u_i|^2, i = i - 1$ go to Step 3 $\}$.
 Else ($i = 4$) $\{$ Compute u_k using (31) and $T_{k-1} = T_k + |r_k - \sum_{j=k}^8 \theta_{kj}u_j|^2, k = i, \dots, 1$,
 then go to Step 6 $\}$.
- 5) If $i = 8$, then terminate; else set $i = i + 1$ and go to Step 7.
- 6) (A valid point is found) Let $d_c = T_0$, save $\hat{\mathbf{u}} = \mathbf{u}$. Then $i = i + 1$ go to Step 7.
- 7) (SE enumeration of level i) Let $u_i = u_i + \Delta_i$, $\Delta_i = -\Delta_i - \text{sign}(\Delta_i)$, then go to Step 4.

Summarizing, in sphere-decoded fast-decodable 2×2 STBCs we have the following complexity reduction:

- 1) We use a 4-dimensional real SD in lieu of the "standard" 8-dimensional real SD.
- 2) The interference term ξ_i vanishes at levels $5 \leq i \leq 8$ vanishes, allowing faster computation of T_i and Δ_i .

Remark 1: (More on decoding complexity) As we have proved *supra*, the worst-case decoding complexity of fast-decodable STBCs is $2M^3$. This can also be obtained from our discussion of the SD algorithm, because: 1) A 4-dimensional real SD (2-dimensional complex SD) requires M^2 branch metric computation, and 2) Alamouti decoding requires $2M$ branch metric computations. However, in practice, the decoding complexity may not exceed $2M^2$, given that one can use two symbol-by-symbol hard decisions on the PAM components to decode in each branch of the 4-dimensional tree.

C. The general structure of fast-decodable 2×2 STBCs

Based on our description of the SD algorithm, we summarize here the design criteria of fast-decodable 2×2 STBCs.

Criterion 1 To reduce the SD search from an 8-dimensional space to a 4-dimensional one, we need $\langle \mathbf{f}_2, \mathbf{e}_1 \rangle = 0$, or equivalently, $\langle \mathbf{f}_2, \mathbf{f}_1 \rangle = 0$. This implies that the code $\mathbf{X}_{1,2}$ must have the Alamouti structure. \square

Criterion 2 To further save computational complexity, we may require $\langle \mathbf{f}_4, \mathbf{e}_3 \rangle = 0$, so that the interference term ξ_i vanishes for $5 \leq i \leq 8$. This can be obtained if $\mathbf{X}_{3,4}$ has the Alamouti structure. Note that this condition is sufficient but not necessary, since the Alamouti structure implies $\langle \mathbf{f}_4, \mathbf{e}_3 \rangle = 0$, but the converse is not true. \square

Criterion 3 (Cubic shaping) To guarantee the cubic shaping of the STBC, the generator matrix \mathbb{G} must satisfy $\mathbb{G}^\dagger \mathbb{G} = \mathbf{I}_8$. \square

In summary:

Remark 2: (General structure of fast-decodable STBC) A STBC of the form (14) has low-complexity decoding if $\mathbf{X}_{1,2}$ has an Alamouti structure and $\mathbf{X}_{3,4}$ has an orthogonal generator matrix. If cubic shaping is required, $\mathbf{X}_{3,4}$ should be chosen so that the column vectors of $\mathbf{X}_{3,4}$ and $\mathbf{X}_{1,2}$ are mutually orthogonal. If in addition $\mathbf{X}_{3,4}$ has the Alamouti structure, then extra savings of computation complexity are available in the SD algorithm. \square

V. NEW STBC FOR 4×2 MIMO

Here we design a fast-decodable 4×2 STBC based on the concepts elaborated upon in the previous sections. We first introduce the relevant definitions.

Definition 11: (Quasi-orthogonal structure) [11] A code such that

$$\mathbf{X} = \begin{bmatrix} s_1 & -s_2^* & -s_3^* & s_4 \\ s_2 & s_1^* & -s_4^* & -s_3 \\ s_3 & -s_4^* & s_1^* & -s_2 \\ s_4 & s_3^* & s_2^* & s_1 \end{bmatrix}$$

where $s_i \in \mathbb{C}$, $i = 1, \dots, 4$, is said to have a quasi-orthogonal structure. Note that a quasi-orthogonal STBC is not full rank and has $r = 2$. \square

Definition 12: (Full-rate, fast-decodable STBC for 4×2 MIMO) A full-rate, fast-decodable STBC for 4×2 MIMO, denoted \mathcal{G}' , has $\kappa = 8$ symbols/codeword, and can be decoded by a 12-dimensional real SD algorithm (rather than the standard 16-dimensional SD). \square

The 4×4 codeword matrix $\mathbf{X} \in \mathcal{G}'$ encodes eight QAM symbols $\mathbf{s} = [s_1, \dots, s_8] \in \mathbb{Z}^8[j]$, and is transmitted by using the channel four times, i.e., $T = 4$. In order to design a STBC satisfying Criteria 1 and 3, we choose a sum structure:

$$\mathbf{X} = \mathbf{X}_{1,2}(s_1, s_2, s_3, s_4) + \mathbf{X}_{3,4}(s_5, s_6, s_7, s_8) \quad (32)$$

where

$$\mathbf{X}_{1,2}(s_1, s_2, s_3, s_4) \triangleq \begin{bmatrix} s_1 & -s_2^* & -s_3^* & s_4 \\ s_2 & s_1^* & -s_4^* & -s_3 \\ s_3 & -s_4^* & s_1^* & -s_2 \\ s_4 & s_3^* & s_2^* & s_1 \end{bmatrix} \quad (33)$$

is quasi-orthogonal, and

$$\mathbf{X}_{3,4}(z_1, z_2, z_3, z_4) \triangleq \mathbf{T} \begin{bmatrix} z_1 & -z_2^* & -z_3^* & z_4 \\ z_2 & z_1^* & -z_4^* & -z_3 \\ z_3 & -z_4^* & z_1^* & -z_2 \\ z_4 & z_3^* & z_2^* & z_1 \end{bmatrix} \quad (34)$$

with

$$\mathbf{T} = \begin{bmatrix} 1 & 0 & 0 & 0 \\ 0 & 1 & 0 & 0 \\ 0 & 0 & -1 & 0 \\ 0 & 0 & 0 & -1 \end{bmatrix} \quad (35)$$

and

$$\begin{bmatrix} z_1 \\ z_2 \\ z_3 \\ z_4 \end{bmatrix} = \mathbf{U} \begin{bmatrix} s_5 \\ s_6 \\ s_7 \\ s_8 \end{bmatrix} \quad (36)$$

where $z_i \in \mathbb{C}$, $i = 1, \dots, 4$, $s_k \in \mathbb{Z}[j]$, $k = 5, \dots, 8$, and

$$\mathbf{U} = [\varphi_1 \mid \varphi_2 \mid \varphi_3 \mid \varphi_4] = \begin{bmatrix} \varphi_{11} & \varphi_{12} & \varphi_{13} & \varphi_{14} \\ \varphi_{21} & \varphi_{22} & \varphi_{23} & \varphi_{24} \\ \varphi_{31} & \varphi_{32} & \varphi_{33} & \varphi_{34} \\ \varphi_{41} & \varphi_{42} & \varphi_{43} & \varphi_{44} \end{bmatrix} \quad (37)$$

is a 4×4 unitary matrix.

Remark 3: (Rank 2) Since the matrix $\mathbf{X}_{1,2}$ has quasi-orthogonal structure, the code is not full rank. In particular it has $r = 2$. \square

Remark 4: (Cubic shaping) Direct computation shows that the matrix \mathbf{T} guarantees cubic shaping. \square

As a consequence of Remark 3, we conduct a search over the matrices \mathbf{U} , leading to the minimum of $\sum_{\delta} A(2, \delta)$, where the terms $A(2, \delta)$ represent the total number of pairwise error events of rank 2 and product distance δ . Since an exhaustive search through all 4×4 unitary matrices is too complex, we focus on those with the form

$$\mathbf{U} = \mathbf{D}\mathbf{P} \quad (38)$$

where $\mathbf{P} \triangleq [\exp(j2\pi\ell n/4)]$ is a 4×4 discrete Fourier transform matrix, $\mathbf{D} = \text{diag}(\exp(j2\pi n_{\ell}/N))$ for some integer N , and $n_{\ell} \in \{0, 1, \dots, N\}$ for $\ell = 1, \dots, 4$.

For 4-QAM signaling, taking $N = 7$ and $n_{\ell} = 1, 2, 5, 6$, we have obtained

$$\mathbf{U} = \begin{bmatrix} 0.31 + 0.39i & 0.31 + 0.39i & 0.31 + 0.39i & 0.31 + 0.39i \\ -0.11 + 0.49i & -0.49 - 0.11i & 0.11 - 0.49i & 0.49 + 0.11i \\ -0.11 - 0.49i & 0.11 + 0.49i & -0.11 - 0.49i & 0.11 + 0.49i \\ 0.31 - 0.39i & -0.39 - 0.31i & -0.31 + 0.39i & 0.39 + 0.31i \end{bmatrix}$$

which yields the minimum $\sum_{\delta} A(2, \delta)$.

Under 4-QAM signaling, we compare the minimum determinants δ_{min} and their associated multiplicities $A(r, \delta_{min})$, as well as the CERs of the above STBC to the following 4×2 codes:

- 1) Code with the structure (32), with \mathbf{U} the 4×4 “perfect” rotation matrix [13];
- 2) The best DjABBA code of [9];
- 3) The “perfect” two-layer code of [8].

Determinant and multiplicity values are shown in Table II. It can be seen that the proposed 4×2 STBC has the minimum $\sum A(2, \delta)$, when compared to the rank-2 code with perfect rotation matrix \mathbf{U} in [13]. The CERs are shown in Fig. 3. The proposed code achieves the best CER up to the CER of 10^{-5} . Due to the diversity loss, the performance curve of the new code and the one of DjABBA has a crossover at CER of 2×10^{-5} .

For 16-QAM signaling, the best matrix \mathbf{U} with $N = 17$ and $n_\ell = 3, 4, 5, 13$ is

$$\mathbf{U} = \begin{bmatrix} 0.22 + 0.44j & 0.22 + 0.44j & 0.22 + 0.44j & 0.22 + 0.44j \\ 0.05 + 0.50j & -0.49 + 0.05j & -0.05 - 0.50j & 0.50 - 0.05j \\ -0.30 - 0.40j & 0.30 + 0.40j & -0.30 - 0.40j & 0.30 + 0.40j \\ 0.05 - 0.50j & -0.50 - 0.05j & -0.05 + 0.50j & 0.50 + 0.05j \end{bmatrix}$$

The performance of this code is compared with that of other codes in Fig. 4. We can see that, at CER= 10^{-4} , it requires an SNR 0.4 dB higher than the best known code of [9], which was not designed for reduced-complexity decoding.

VI. LOW -COMPLEXITY DECODING OF THE 4×2 CODE

Let $\mathbf{Y} = [n_{\ell n}] \in \mathbb{C}^{2 \times 4}$, $\mathbf{H} = [h_{\ell n}] \in \mathbb{C}^{2 \times 4}$, and $\mathbf{N} = [n_{\ell n}] \in \mathbb{C}^{2 \times 4}$. Vectorizing, and conjugating some of the received vector components, we can write

$$\mathbf{y} \triangleq \mathbf{F}^{(*)} \mathbf{s} + \mathbf{n} \tag{39}$$

where

$$\begin{aligned} \mathbf{y} &\triangleq [y_{11}, y_{12}^*, y_{13}^*, y_{14}, y_{21}, y_{22}^*, y_{23}^*, y_{24}]^T \\ \mathbf{n} &\triangleq [n_{11}, n_{12}^*, n_{13}^*, n_{14}, n_{21}, n_{22}^*, n_{23}^*, n_{24}]^T \\ \mathbf{s} &\triangleq [s_1, s_2, s_3, s_4, s_5, s_6, s_7, s_8]^T \end{aligned}$$

and

$$\mathbf{F}^{(*)} \triangleq [\mathbf{F}_1 \mid \mathbf{F}_2] \tag{40}$$

where

$$\mathbf{F}_1 = [\mathbf{f}_1 \mid \mathbf{f}_2 \mid \mathbf{f}_3 \mid \mathbf{f}_4] = \begin{bmatrix} h_{11} & h_{12} & h_{13} & h_{14} \\ h_{12}^* & -h_{11}^* & h_{14}^* & -h_{13}^* \\ h_{13}^* & h_{14}^* & -h_{11}^* & -h_{12}^* \\ h_{14} & -h_{13} & -h_{12} & h_{11} \\ h_{21} & h_{22} & h_{23} & h_{24} \\ h_{22}^* & -h_{21}^* & h_{24}^* & -h_{23}^* \\ h_{23}^* & h_{24}^* & -h_{21}^* & -h_{22}^* \\ h_{24} & -h_{23} & -h_{22} & h_{21} \end{bmatrix}$$

and $\mathbf{F}_2 = [\mathbf{f}_5 \mid \mathbf{f}_6 \mid \mathbf{f}_7 \mid \mathbf{f}_8]$ with

$$\mathbf{f}_5 = \mathbf{M}\boldsymbol{\varphi}_1 \quad \mathbf{f}_6 = \mathbf{M}\boldsymbol{\varphi}_2 \quad \mathbf{f}_7 = \mathbf{M}\boldsymbol{\varphi}_3 \quad \mathbf{f}_8 = \mathbf{M}\boldsymbol{\varphi}_4$$

where

$$\mathbf{M} = \begin{bmatrix} h_{11} & h_{12} & -h_{13} & -h_{14} \\ h_{12}^* & -h_{11}^* & -h_{14}^* & h_{13}^* \\ -h_{13}^* & -h_{14}^* & -h_{11}^* & -h_{12}^* \\ -h_{14} & h_{13} & -h_{12} & h_{11} \\ h_{21} & h_{22} & -h_{23} & -h_{24} \\ h_{22}^* & -h_{21}^* & -h_{24}^* & h_{23}^* \\ -h_{23}^* & -h_{24}^* & -h_{21}^* & -h_{22}^* \\ -h_{24} & h_{23} & -h_{22} & h_{21} \end{bmatrix}$$

The QR decomposition of $\mathbf{F}^{(*)}$ yields $\mathbf{F}^{(*)} = \mathbf{Q}\mathbf{R}$, where $\mathbf{Q} \in \mathbb{C}^{8 \times 8}$ is a unitary matrix and $\mathbf{R} \in \mathbb{C}^{8 \times 8}$ is an upper-triangular matrix:

$$\mathbf{Q} = [\mathbf{e}_1 \mid \mathbf{e}_2 \mid \mathbf{e}_3 \mid \mathbf{e}_4 \mid \mathbf{e}_5 \mid \mathbf{e}_6 \mid \mathbf{e}_7 \mid \mathbf{e}_8]$$

$$\mathbf{R} = \begin{bmatrix} \|\mathbf{d}_1\| & \langle \mathbf{f}_2, \mathbf{e}_1 \rangle & \langle \mathbf{f}_3, \mathbf{e}_1 \rangle & \cdots & \langle \mathbf{f}_8, \mathbf{e}_1 \rangle \\ 0 & \|\mathbf{d}_2\| & \langle \mathbf{f}_3, \mathbf{e}_2 \rangle & \cdots & \langle \mathbf{f}_8, \mathbf{e}_2 \rangle \\ 0 & 0 & \|\mathbf{d}_3\| & \cdots & \langle \mathbf{f}_8, \mathbf{e}_3 \rangle \\ \vdots & \ddots & \ddots & \ddots & \vdots \\ 0 & 0 & 0 & \cdots & \|\mathbf{d}_8\| \end{bmatrix}$$

Direct computation shows that \mathbf{R} has the following properties:

- 1) $\langle \mathbf{f}_2, \mathbf{e}_1 \rangle = 0$

- 2) $\mu \triangleq \|\mathbf{d}_i\|^2 = \sum_{i=1}^2 \sum_{j=1}^4 |h_{ij}|^2$
- 3) $\langle \mathbf{f}_4, \mathbf{e}_1 \rangle = -\langle \mathbf{f}_3, \mathbf{e}_2 \rangle = \Phi_1 / \sqrt{\mu}$ where $\Phi_1 \triangleq 2\Re(h_{11}^* h_{14} + h_{21} h_{24}^* - h_{12} h_{13}^* - h_{22} h_{23}^*)$
- 4) $\gamma \triangleq \|\mathbf{d}_i\|^2 = \mu - \Phi_1^2 / \mu$ with $i = 3, 4$
- 5)

$$\mathbf{R} = \begin{bmatrix} \mathbf{S}_1 & \mathbf{S}_2 \\ \mathbf{0}_{4 \times 4} & \mathbf{S}_3 \end{bmatrix} \quad (41)$$

where

$$\mathbf{S}_1 = \begin{bmatrix} \sqrt{\mu} & 0 & 0 & \Phi_1 \\ 0 & \sqrt{\mu} & -\Phi_1 & 0 \\ 0 & 0 & \sqrt{\gamma} & 0 \\ 0 & 0 & 0 & \sqrt{\gamma} \end{bmatrix} \quad (42)$$

and

$$\mathbf{S}_2 = \begin{bmatrix} \langle \mathbf{f}_5, \mathbf{e}_1 \rangle & \langle \mathbf{f}_6, \mathbf{e}_1 \rangle & \langle \mathbf{f}_7, \mathbf{e}_1 \rangle & \langle \mathbf{f}_8, \mathbf{e}_1 \rangle \\ \langle \mathbf{f}_5, \mathbf{e}_2 \rangle & \langle \mathbf{f}_6, \mathbf{e}_2 \rangle & \langle \mathbf{f}_7, \mathbf{e}_2 \rangle & \langle \mathbf{f}_8, \mathbf{e}_2 \rangle \\ \langle \mathbf{f}_5, \mathbf{e}_3 \rangle & \langle \mathbf{f}_6, \mathbf{e}_3 \rangle & \langle \mathbf{f}_7, \mathbf{e}_3 \rangle & \langle \mathbf{f}_8, \mathbf{e}_3 \rangle \\ \langle \mathbf{f}_5, \mathbf{e}_4 \rangle & \langle \mathbf{f}_6, \mathbf{e}_4 \rangle & \langle \mathbf{f}_7, \mathbf{e}_4 \rangle & \langle \mathbf{f}_8, \mathbf{e}_4 \rangle \end{bmatrix} \quad (43)$$

$$\mathbf{S}_3 = \begin{bmatrix} \|\mathbf{d}_5\| & \langle \mathbf{f}_6, \mathbf{e}_5 \rangle & \langle \mathbf{f}_7, \mathbf{e}_5 \rangle & \langle \mathbf{f}_8, \mathbf{e}_5 \rangle \\ 0 & \|\mathbf{d}_6\| & \langle \mathbf{f}_7, \mathbf{e}_6 \rangle & \langle \mathbf{f}_8, \mathbf{e}_6 \rangle \\ 0 & 0 & \|\mathbf{d}_7\| & \langle \mathbf{f}_8, \mathbf{e}_7 \rangle \\ 0 & 0 & 0 & \|\mathbf{d}_8\| \end{bmatrix} \quad (44)$$

□

After the QR decomposition, (39) becomes

$$\mathbf{y} = \mathbf{QRs} + \mathbf{n} \quad (45)$$

and, pre-multiplying by \mathbf{Q}^\dagger , we obtain

$$\mathbf{r} = \mathbf{Q}^\dagger \mathbf{y} = \mathbf{Rs} + \mathbf{w} \quad (46)$$

Let $\mathbf{r} = [r_1, \dots, r_8]^T$, and $\mathbf{w} \triangleq \mathbf{Q}^\dagger \mathbf{n} = [w_1, \dots, w_8]^T$. Separating real and imaginary parts in (46), we obtain

$$\tilde{\mathbf{r}} = \tilde{\mathbf{R}}\tilde{\mathbf{s}} + \tilde{\mathbf{w}} \implies \mathbf{v} = \Theta \mathbf{u} + \tilde{\mathbf{w}} \quad (47)$$

where

$$\mathbf{v} \triangleq [v_1, \dots, v_{16}]^T = \tilde{\mathbf{r}}$$

$$\mathbf{u} \triangleq [u_1, \dots, u_{16}]^T = \tilde{\mathbf{s}}$$

$$\tilde{\mathbf{w}} \triangleq [\tilde{w}_1, \dots, \tilde{w}_8]^T$$

and $\Theta \triangleq (\theta_{ij}) \triangleq \check{\mathbf{R}}$, $i, j = 1, \dots, 16$.

Sphere decoding is now used to obtain

$$\hat{\mathbf{u}} = \arg \min_{\mathbf{u} \in \mathcal{X}} \|\mathbf{v} - \Theta \mathbf{u}\|_F^2 \quad (48)$$

where $\hat{\mathbf{u}} = \{\hat{u}_i\}$ with $i = 1, \dots, 16$ and $\hat{u}_i \in \mathcal{X}$. Standard real SD of 4×2 codes requires 16 levels of tree search. With our code, the quasi-orthogonal structure of the codeword matrix allows us to use only a 12-level tree search, as shown in the following.

Consider again SE enumeration [17] to decode \mathbf{u}_{12}^{16} . This starts at level i :

$$S_i(u_i) = \lfloor (v_i - \xi_i) / \theta_{ii} \rfloor \in \mathcal{X} \quad i = 16, \dots, 9 \quad (49)$$

where $\xi_{16} = 0$. In (49), we define the *interference term* on level i from upper levels j as

$$\xi_i \triangleq \sum_{j=i+1}^{16} \theta_{ij} u_j, \quad i = 16, \dots, 9 \quad (50)$$

Since \mathbf{S}_3 is not the null matrix, we have nonzero interference terms. Define, for future use,

$$\Delta_i \triangleq \text{sign}(v_i - \xi_i - \theta_{ii} u_i)$$

The SE enumeration is the same as with 2×2 codes. Note that at the decoding level $9 \leq i \leq 16$, each branch corresponds to the values of symbol u_i , and is labeled by the branch metric

$$d_i(\mathbf{u}_9^{16}) \triangleq |v_i - \xi_i - \theta_{ii} u_i|^2 \quad 9 \leq i \leq 16 \quad (51)$$

The corresponding path metric is given by

$$T_{i-1} \triangleq \sum_{j=i}^{16} d_j(\mathbf{u}_j^{16}) \quad (52)$$

When the SD reaches the decoding-tree levels $i \leq 8$, a first complexity reduction is available. Given the vector \mathbf{u}_9^{16} , ξ_i can be computed for all the remaining level $i = 1, \dots, 8$:

$$\xi_i \triangleq \sum_{j=9}^{16} \theta_{ij} u_j$$

which saves a few multiplications in the computation of ξ_i in (50). Next, we proceed with the standard SD searching procedure to find \mathbf{u}_5^8 . We obtain the remaining symbols as

$$\begin{aligned}
 S_1(u_1) &= \left\lfloor \frac{(v_1 - \xi_1 - \frac{\Phi_1}{\sqrt{\mu}}u_7)}{\mu} \right\rfloor \in \mathcal{X} \\
 S_2(u_2) &= \left\lfloor \frac{(v_2 - \xi_2 - \frac{\Phi_1}{\sqrt{\mu}}u_8)}{\mu} \right\rfloor \in \mathcal{X} \\
 S_3(u_3) &= \left\lfloor \frac{(v_3 - \xi_3 + \frac{\Phi_1}{\sqrt{\mu}}u_5)}{\mu} \right\rfloor \in \mathcal{X} \\
 S_4(u_4) &= \left\lfloor \frac{(v_4 - \xi_4 + \frac{\Phi_1}{\sqrt{\mu}}u_6)}{\mu} \right\rfloor \in \mathcal{X}
 \end{aligned} \tag{53}$$

We say that the remaining four-level tree search in SD is not necessary, or, equivalently, that a 12-dimensional real SD replaces the standard 16-dimensional one.

After obtaining \mathbf{u}_1^8 , we have a valid vector $\mathbf{u} = [\mathbf{u}_1^8, \mathbf{u}_9^{16}]$. We then compute the corresponding branch and path metrics in (29) and (30), respectively. This completes the search of one path in the 12-dimensional bounded tree. The detailed decoding algorithm is given below.

- 1) (Input) Input Φ_1 and α .
- 2) (Initialization) Set $i = 16$, $T_{16} = 0$, $\xi_{16} = 0$, and $d_c = C_0$ (current squared radius of the sphere).
- 3) Set $u_i = \lfloor (v_i - \xi_i)/\theta_{ii} \rfloor$ and $\Delta_i = \text{sign}(v_i - \xi_i - \theta_{ii}u_i)$.
- 4) (Main step of SD) If $d_c < T_i + |v_i - \xi_i - \theta_{ii}u_i|^2$, then go to Step 5 (outside of the sphere). Else if u_i is not in \mathcal{X} go to Step 7 (inside of the sphere, outside of the signal set).
Else (inside of the sphere, inside of the signal set)
 - If $i \geq 9$ then $\{ T_{i-1} = T_i + |v_i u - \xi_i - \theta_{ii}u_i|^2, \xi_{i-1} = \sum_{j=i+1}^{16} \theta_{ij}u_j, i = i - 1$ go to Step 3 }.
 - Else if $(i \geq 5)$ then $\{ T_{i-1} = T_i + |v_i u - \xi_i - \theta_{ii}u_i|^2, \xi_{i-1} = \sum_{j=9}^{16} \theta_{ij}u_j, i = i - 1$ go to Step 3 }.
 - Else $(i = 4)$ {Compute u_k using (53) and $T_{k-1} = T_k + |v_k - \sum_{j=k}^m \theta_{kj}u_j|^2, k = i, \dots, 1$, then go to Step 6 }.
- 5) If $i = 16$ then terminate; else set $i = i + 1$ and go to Step 7.
- 6) (A valid vector is found) Let $d_c = T_0$, save $\hat{\mathbf{u}} = \mathbf{u}$. Then $i = i + 1$ go to Step 7.
- 7) (SE enumeration of level i) Let $u_i = u_i + \Delta_i$, $\Delta_i = -\Delta_i - \text{sign}(\Delta_i)$, go to Step 4.

Summarizing, we observe the following reductions of decoding complexity: (1) We use a 12-dimensional real SD to find \mathbf{u}_5^{16} . Then, we subtract the interference terms from \mathbf{u}_5^{16} (see (53)). Finally, the partial symbol vector \mathbf{u}_1^4 can be computed directly. We see that the standard 16-dimensional real SD is not necessary. (2) The interference term ξ_i at the i th level $i = 1, \dots, 8$, admits simple calculation.

In other terms, we observe that the worst-case decoding complexity of fast-decodable STBCs is $2M^7$, as compared to a standard SD complexity M^8 . This is due to the fact that: (1) A 12-dimensional real SD (6-dimensional complex SD) requires M^6 branch metric computations, and (2) In each branch of the 6-dimensional tree, part of decoding can be treated as Alamouti decoding, resulting in $2M$ branch metric computations. Moreover, if two hard-decision, symbol-by-symbol decoding steps in each branch of the 6-dimensional real SD are taken, the decoding complexity does not exceed $2M^6$.

VII. CONCLUSION

In this paper we study, under a unified framework, two families of full-rate, full-diversity 2×2 STBCs. We compare their minimum determinant, CER performance, and shaping property, and we examine how both families allow low-complexity ML decoding. Detailed examination of an SD algorithm shows that the SD search can be reduced from a 8- to a 4-dimensional space, and that the interference term vanishes at decoding levels greater than 5. We also derive design criteria of fast-decodable STBCs for 2×2 MIMO.

These design criteria are then extended to the construction of a fast-decodable 4×2 code. Combining algebraic and quasi-orthogonal STBC structures, a new code is found that outperforms any known 4×2 code for 4-QAM signaling. A reduced-complexity SD algorithm enables using only a 12-dimensional real SD, rather than the standard 16-dimensional one. In addition, the computation cost of the interference terms can be reduced in the decoding levels below 8.

REFERENCES

- [1] S. M. Alamouti, "A simple transmit diversity technique for wireless communications," *IEEE J. Select. Areas Commun.*, vol. 16, no. 8, pp. 1451–1458, October 1998.
- [2] J.-C. Belfiore, G. Rekaya, and E. Viterbo, "The Golden Code: A 2×2 full-rate space-time code with non-vanishing determinants," *IEEE Trans. Inform. Theory*, vol. 51, no. 4, pp. 1432–1436, April 2005.

- [3] M.O. Damen, A. Chkeif, and J.-C. Belfiore, "Lattice code decoder for space–time codes," *IEEE Communication Letters*, vol. 4, no. 5, pp. 161–163, May 2000.
- [4] M.O. Damen, H. El Gamal, and G. Caire, "On maximum-likelihood detection and the search for the closest lattice point," *IEEE Trans. Inform. Theory*, vol. 49, no. 10, pp. 2389–2402, October 2003.
- [5] H. El Gamal and M. O. Damen, "Universal space–time codes," *IEEE Trans. Inform. Theory*, vol. 49, no. 5, pp. 1097–1119, May 2003.
- [6] J.-C. Guey, M.P. Fitz, M.R. Bell, and W.-Y. Guo, "Signal design for transmitter diversity wireless communication Systems over Rician fading channels," *IEEE Trans. Commun.*, vol. 47, no. 4, pp. 527–537, 1999.
- [7] P. Elia, K.R. Kumar, S.A. Pawar, P.V. Kumar, and H.-F. Lu, "Explicit space–time codes that achieve the diversity-multiplexing gain tradeoff," *IEEE Int. Symp. Inform. Theory (ISIT 2005)*, pp. 896–900, Adelaide, Australia, September 4–9, 2005.
- [8] Y. Hong, E. Viterbo, and J.-C. Belfiore, "A space–time block coded multiuser MIMO downlink transmission scheme," in Proc. *IEEE Int. Symp. Inform. Theory (ISIT 2006)*, pp. 257–261, Seattle, WA, USA, June–July, 2006.
- [9] A. Hottinen and O. Tirkkonen, "Precoder designs for high rate space–time block codes," in Proc. *Conference on Information Sciences and Systems*, Princeton, NJ, March 17–19, 2004.
- [10] A. Hottinen, O. Tirkkonen and R. Wichman, "Multi-antenna Transceiver Techniques for 3G and Beyond," WILEY publisher, UK.
- [11] H. Jafarkhani, "A quasi-orthogonal space–time block code," in *IEEE Commun. Letters*, vol. 49, no. 1, pp. 1–4, January 2001.
- [12] E. G. Larsson and P. Stoica, *Space-Time Block Coding for Wireless Communications*. Cambridge, U.K.: Cambridge University Press, 2003.
- [13] F. Oggier, G. Rekaya, J.-C. Belfiore, and E. Viterbo, "Perfect space–time block codes," *IEEE Trans. Inform. Theory*, vol. 52, n. 9, pp. 3885–3902, September 2006.
- [14] F. Oggier and E. Viterbo, "Algebraic Number Theory and Code Design for Rayleigh Fading Channels", in *Foundations and Trends in Communications and Information Theory*, vol. 1, pp. 333–415, 2004.
- [15] J. Paredes, A.B. Gershman, and M. G. Alkhanari, "A 2×2 space–time code with non-vanishing determinants and fast maximum likelihood decoding," in Proc *IEEE International Conference on Acoustics, Speech, and Signal Processing (ICASSP 2007)*, Honolulu, Hawaii, USA, pp. 877–880, April 2007.
- [16] M. Samuel and M. P. Fitz, "Reducing the detection complexity by using 2×2 multi-strata space–time codes," in Proc *IEEE Int. Symp. Inform. Theory (ISIT 2007)*, pp. 1946–1950, Nice, France, June 2007.
- [17] C. P. Schnorr and M. Euchner, "Lattice basis reduction: Improved practical algorithms and solving subset sum problems," *Math Programming*, vol. 66, pp. 181–191, 1994.
- [18] B. A. Sethuraman, B. S. Rajan, and V. Shashidhar, "Full-diversity, high-rate space–time block codes from division algebras," *IEEE Trans. Inform. Theory*, vol. 49, pp. 2596–2616, October 2003.
- [19] S. Sezginer and H. Sari, "A full-rate full-diversity 2×2 space–time code for mobile Wimax Systems," in Proc. *IEEE International Conference on Signal Processing and Communications*, Dubai, July 2007.
- [20] V. Tarokh, H. Jafarkhani, A. R. Calderbank, "Space–time block codes from orthogonal designs," *IEEE Trans. Inform.*

Theory, vol. 45, no. 5, pp. 1456–1467, July 1999.

- [21] V. Tarokh, N. Seshadri and A. R. Calderbank, "Space–time codes for high data rate wireless communications: performance criterion and code construction," *IEEE Trans. Inform. Theory*, vol. 44, no. 2, pp. 744–765, March 1998.
- [22] O. Tirkkonen and A. Hottinen, "Square-matrix embeddable space–time block codes for complex signal constellations," in *IEEE Trans. Inform. Theory*, vol. 48, no. 2, , pp. 384–395, February 2002.
- [23] O. Tirkkonen and R. Kashaev, "Combined information and performance optimization of linear MIMO modulations," in *Proc IEEE Int. Symp. Inform. Theory (ISIT 2002)*, Lausanne, Switzerland, p. 76, June 2002.
- [24] E. Viterbo and E. Biglieri, "A universal lattice decoder," in *GRETSI 14-ème Colloque*, Juan-les-Pins, France, September 1993.
- [25] E. Viterbo and J. Boutros, "A universal lattice code decoder for fading chanel," *IEEE Trans. Inform. Theory*, vol. 45, pp. 1639–1642, July 1999.

\mathcal{G}	δ_{\min} for 4-QAM	δ_{\min} for 16-QAM	δ_{\min} for 64-QAM
1st Family	2.2857	2.2857	2.2857
2nd Family	1.9973	1.9796	1.8784
Golden Code	3.2	3.2	3.2

TABLE I

THE MINIMUM DETERMINANTS δ_{\min} OF THE GOLDEN CODE AND TWO FAMILIES OF FAST-DECODABLE STBCs WITH 4-, 16-, AND 64-QAM SIGNALING.

Tables

- 1) The minimum determinants δ_{\min} of the Golden code and two families of fast-decodable STBCs with 4-, 16-, and 64-QAM signaling.
- 2) Minimum determinants and the associate multiplicities of STBCs for a 4×2 MIMO system with 4-QAM signaling.

Figures

- 1) Comparison of the CER of the best codes in the two fast-decodable STBC families and the Golden code with 4-QAM signaling for 2×2 MIMO.
- 2) Comparison of the CER of the best codes in the two fast-decodable STBC families and the Golden code with 16-QAM signaling for 2×2 MIMO.
- 3) Comparison of the CER of different STBCs for a 4×2 MIMO system with 4-QAM signaling.
- 4) Comparison of the CER of different STBCs for a 4×2 MIMO system with 16-QAM signaling.

Codes	δ_{\min}	Multiplicities
New STBC	0	$\sum_{\delta} A(2, \delta) = 160$
Perfect Code U matrix	0	$\sum_{\delta} A(2, \delta) = 560$
DjABBA	0.8304	$A(4, 0.8304) = 770$
Two-Layers Perfect Code	0.0016	$A(4, 0.0016) = 128$

TABLE II

MINIMUM DETERMINANTS OF 4×2 STBCS WITH 4-QAM SIGNALING

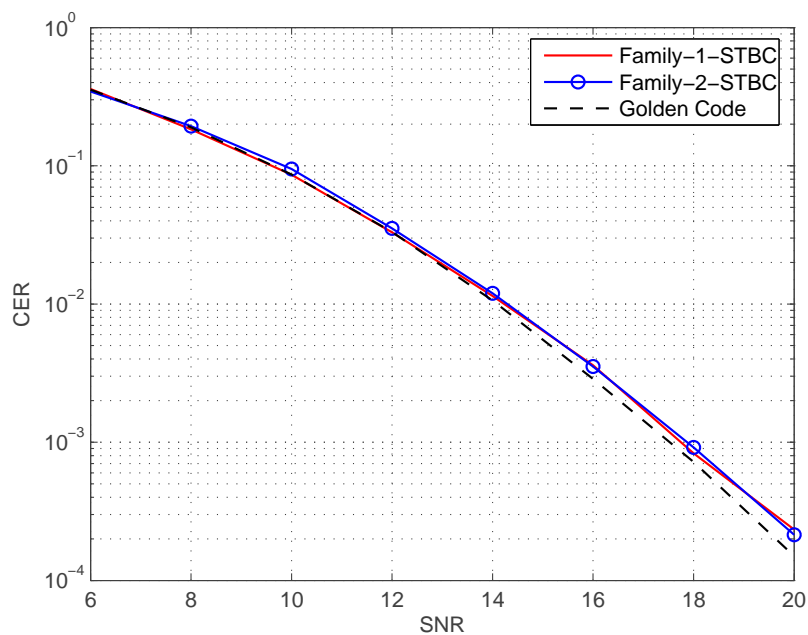


Fig. 1. Comparison of the CER of the best 2×2 codes in two fast-decodable STBC families and of the Golden code with 4-QAM signaling.

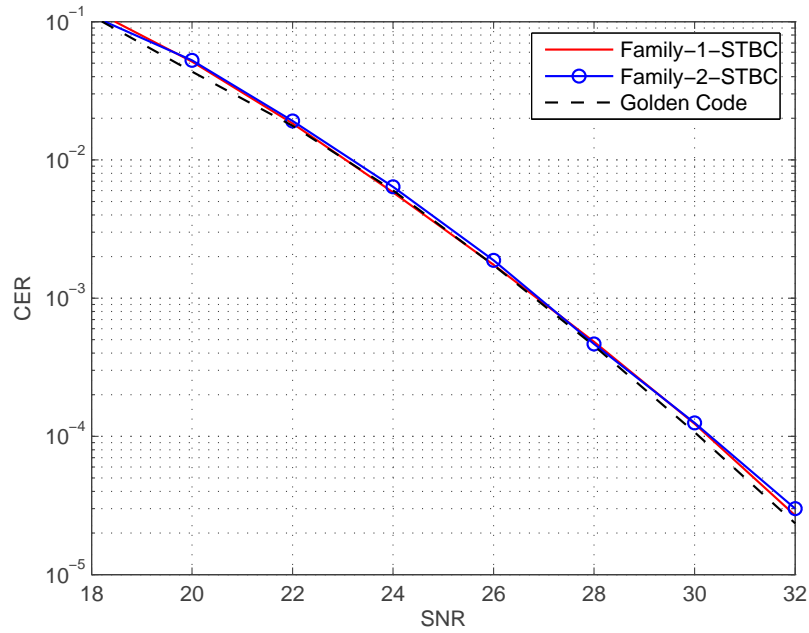


Fig. 2. Comparison of the CER of the best 2×2 codes in two fast-decodable STBC families and of the Golden code with 16-QAM signaling.

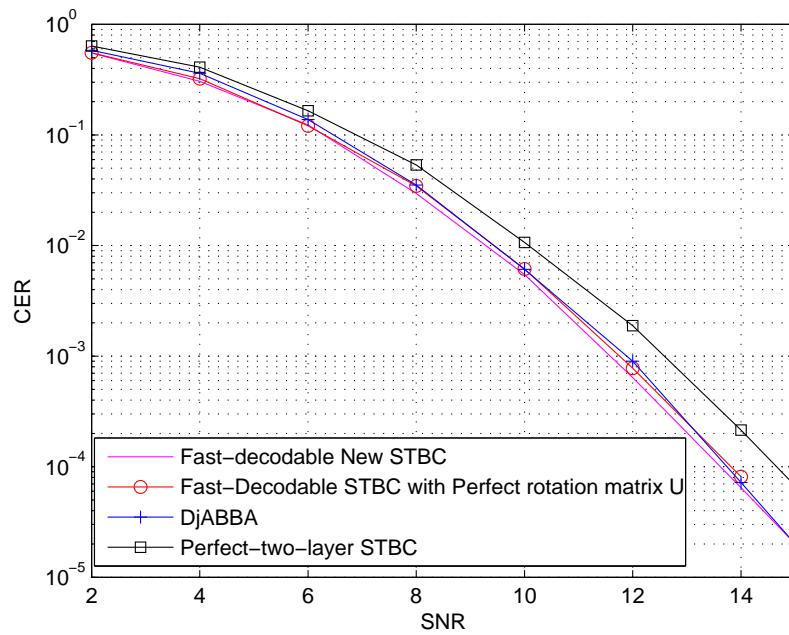


Fig. 3. Comparison of the CER of different 4×2 STBCs with 4-QAM signaling.

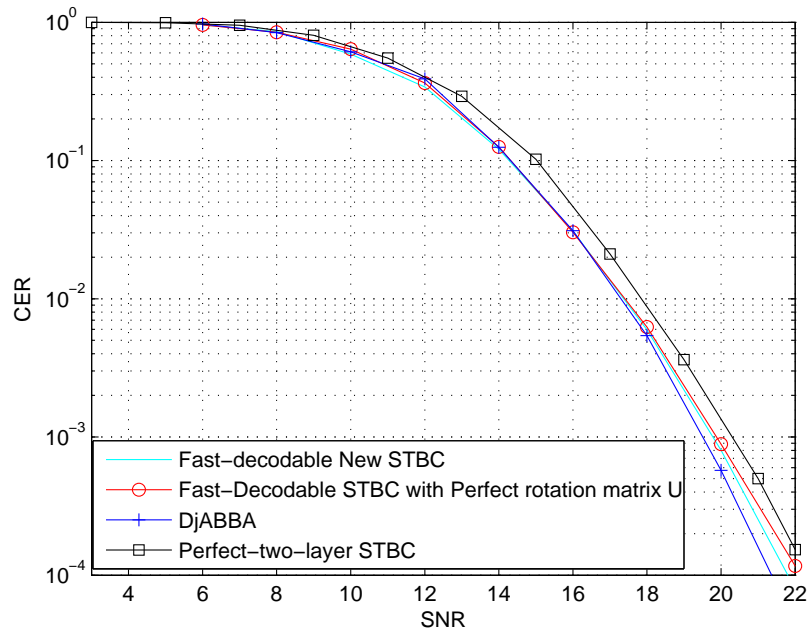


Fig. 4. Comparison of the CER of different 4×2 STBCs with 16-QAM signaling.